

Failure Mechanisms of Ti-Al₃Ti metal-Intermetallic Laminate Composites Under High-Speed Impact

Fan Xueling¹, Yuan Meini², Qin Qiang³

¹ State Key Laboratory for Strength and Vibration of Mechanical Structures, Xi'an Jiaotong University, Xi'an 710049, China; ² North University of China, Taiyuan 030051, China; ³ Aircraft Strength Research Institute, Aviation Industry Corporation of China, Xi'an 710065, China

Abstract: The penetration process of Ti-Al₃Ti metal-intermetallic laminate composites impacted by a projectile was numerically investigated. The ballistic performance, stress distribution, failure and energy absorbing mechanisms of Ti-Al₃Ti metal-intermetallic laminate composites under high-speed impact were examined in detail. The results show that Ti-Al₃Ti metal-intermetallic laminate composites under high-speed impact is mostly under tensile stress, since the compressive wave is reflected back as a tensile wave. During projectile penetration, transverse, inclined, and vertical cracks are formed in the Al₃Ti phase, which can dramatically absorb the kinetic energy of projectile.

Key words: metal-intermetallic laminate composites; finite element method; high-speed impact; failure

Ti-Al₃Ti metal-intermetallic laminate (MIL) composites are composed of alternating layers of Ti and Al₃Ti. The intermetallic phases Al₃Ti provide high hardness and compressive strength, while the ductile metal Ti layers give necessary ductility, which serve to constrain and connect the Al₃Ti layers together^[1,2]. Ti-Al₃Ti MIL composites have a great potential for lightweight structural-armor materials due to their combination of high hardness, compressive strength and some level of ductility at a lower density than monolithic titanium^[3-5].

Over the last two decades, researchers have concentrated on the fabrication as well as improving the mechanical properties and fracture resistance of Ti-Al₃Ti MIL composites^[6-8]. However, limited researches were conducted on characterizing the ballistic impact behaviors and failure mechanisms of Ti-Al₃Ti MIL composites. Harach et al.^[9] demonstrated that compared with the high-strength steel, the same ballistic performance could be obtained for the Ti-Al₃Ti MIL composite with approximately half of density. Randow and Gazona^[10] used the smoothed particle hydrodynamic method to study the ballistic damage tolerance of MIL composites under an impact speed of 1000 m/s. Zelepugin et al.^[11] simulated the

impact process between the projectile and MIL composites, and their results indicated that the penetration depth of MIL composites was strongly dependent upon the volume fraction of Ti. Cao et al.^[12] numerically investigated the failure mode and damage mechanisms of Ti-Al₃Ti MIL composites under ballistic impact. It is critical to acquire more information on the ballistic impact behavior of Ti-Al₃Ti MIL composites, which leads to better design and application in structural-armor materials.

In this paper, finite element analysis was adopted to investigate the penetration process of Ti-Al₃Ti MIL composites impacted by the projectile. Moreover, the stress distribution, the failure mechanism and the energy absorbing mechanism of Ti-Al₃Ti MIL composites during the impact process of the tungsten projectile were studied.

1 Finite Element Modeling of Ballistic Impact Tests

A two dimensional (2D) axi-symmetric model was adopted to analyze the ballistic impact on Ti-Al₃Ti MIL composites. The 2D axi-symmetric model consisted of a Ti-Al₃Ti MIL composite target and a projectile with an

Received date: September 15, 2017

Foundation item: National Key Basic Research Development Program of China ("973" Program) (2013CB035700); National Natural Science Foundation of China (11472204, U1530259)

Corresponding author: Fan Xueling, Ph. D., Associate Professor, State Key Laboratory for Strength and Vibration of Mechanical Structures, School of Aerospace Engineering, Xi'an Jiaotong University, Xi'an 710049, P. R. China, Tel: 0086-29-82667864, E-mail: fanxueling@mail.xjtu.edu.cn

Copyright © 2018, Northwest Institute for Nonferrous Metal Research. Published by Elsevier BV. All rights reserved.

initial velocity, as shown in Fig.1. The Ti-Al₃Ti MIL composites consisted of 18 layers of Ti and 17 layers of Al₃Ti with thickness of ~0.23 and ~0.94 mm, respectively. The total length and diameter of the spherical-nosed projectile was 23.0 and 6.15 mm, respectively, which was made of a tungsten alloy with a density of ~18.5 g/cm³. The initial impact velocity of the projectile was 900 m/s.

The tungsten alloy projectile, Ti and Al₃Ti layers in MIL composites were meshed with 2D axi-symmetric quadratic shell. The size of projectile element was about 0.5 mm×0.5 mm, while element size of the every layer of composite target was about 0.5 mm × 0.2 mm. The total numbers of elements were 58865 and 59421, respectively. Mesh sensitivity studies revealed that further refinement does not significantly improve the accuracy of the calculations but sacrifices longer computational time.

The finite element model considered realistic boundary conditions during the perforation process. A zero value is imposed to the displacement in the z-direction and rotations in x and y directions for all the elements, and the edges of composite layers were fixed.

The CONTACT_ERODING_SURFACE_TO_SURFACE contact model was defined between the projectile and Ti-Al₃Ti MIL composite target. This model allowed elements to be eroded from both of the projectile and target when certain failure criteria were met. As every layer of Ti-Al₃Ti MIL composite target was treated as an individual part in LS-DYNA, the interactions between each layer of Ti-Al₃Ti MIL composite were defined as CONTACT_AUTOMATIC_SURFACE_TO_SURFACE_TIEBREAK.

In the simulation, the titanium layers as well as the tungsten alloy projectile were modeled using the Johnson-Cook (JC) material model and the Johnson-Cook fracture criterion. Their material parameters were given in Table 1^[13]. In the JC model, the equivalent stress σ_{eq} can be expressed as^[14]:

$$\sigma_{eq} = [A + B\varepsilon^n][1 + C \ln \varepsilon][1 - T^{*m}] \quad (1)$$

where A , B , n , C and m are the material constants, ε is the equivalent plastic strain, and the dimensionless plastic

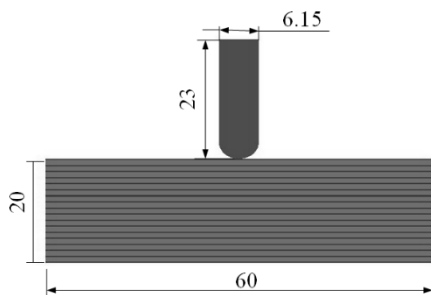


Fig.1 2D axi-symmetric model of projectile and Ti-Al₃Ti MIL composites target (mm)

strain rate $\dot{\varepsilon}^*$ is equal to $\dot{\varepsilon}/\dot{\varepsilon}_0$. The homologous temperature T^* is defined as follows:

$$T^* = (T - 298) / (T_{melt} - 298) \quad (2)$$

where T and T_{melt} is absolute temperature and melting temperature, respectively.

The damage parameter, D , ($0 < D < 1$) in the JC fracture criterion describes the degree of damage, which is written as follows:

$$D = \sum (\Delta \varepsilon / \varepsilon_f) \quad (3)$$

The equivalent fracture strain is given by:

$$\varepsilon_f = [D_1 + D_2 \exp(D_3 \sigma^*)][1 + D_4 \ln \varepsilon][1 + D_5 T^*] \quad (4)$$

where D_1 , D_2 , D_3 , D_4 and D_5 are material constants, σ_m is the hydrostatic stress, and $\sigma^* = \sigma_m / \sigma_{eq}$ is the stress triaxiality.

When using the JC model to simulate the material's dynamic response, Gruneisen's equation of state was necessary to describe the relationship between pressure and volume difference. Gruneisen's equation of state has the following form^[12]:

$$P = \frac{\rho_0 C^2 \mu [1 + (1 - \frac{\gamma_0}{2})\mu - \frac{\alpha}{2} \mu^2]}{[1 - (S_1 - 1)\mu - S_2 \frac{\mu^2}{\mu + 1} - S_3 \frac{\mu^2}{(\mu + 1)^2}]^2} \quad (5)$$

where P is pressure, μ is the volume difference, C is material sound velocity and S_1 , S_2 and S_3 are fluid state equation coefficients.

The Johnson-Holmquist-Ceramics (JH-2) model was applicable for establishing the constitutive relation of intermetallic Al₃Ti. Table 2 lists the necessary material constants for Al₃Ti used in the JH-2 model, some of which were taken from aluminum nitride^[15] due to lack of the data for the Al₃Ti intermetallic. The constitutive data of Al₃Ti matrix was found and the effectiveness of these parameters was confirmed by Li et al.^[16]

When using the JH-2 model to simulate the intermetallic Al₃Ti response, the damage parameter D for the intermetallic Al₃Ti was defined as the ratio of equivalent plastic strain increment to fracture strain. Different strength models corresponding to different damage degrees (Fig.2) need to be employed as follows^[17]:

$$\sigma_i^* = A(p^* + T^*)^N (1 + C \ln \dot{\varepsilon}) \quad D = 0 \quad (6)$$

$$\sigma_f^* = B p^{*m} (1 + C \ln \dot{\varepsilon}) \quad D = 1 \quad (7)$$

$$\sigma^* = \sigma_i^* - D(\sigma_i^* - \sigma_f^*) \quad D \in (0, 1) \quad (8)$$

Where the parameters A , N , C , B and m in JH-2 model are material constants measured by quasi-static and dynamic compression tests, and p^* and T^* are current and maximum hydrostatic pressures, respectively. Both hydrostatic pressures are normalized by the pressure at the Hugoniot elastic limit (HEL). The current material strength (σ^*) is dependent upon its initial strength (σ_i^*) and fracture strength (σ_f^*). All the strengths mentioned above are normalized by equivalent stress at the HEL measured by plate impact tests.

Table 1 Parameters of tungsten and titanium materials in Johnson-Cook model^[13]

Material	ρ	E/GPa	E	PR	$A/\times 10^{-2}$	$B/\times 10^{-2}$	N	C	M	T_M	T_R	EPSO
Tungsten	18.50	1.60	3.10	0.30	1.506	0.177	0.12	0.016	1.1	1752	293	1.0×10^{-6}
Titanium	4.428	0.434	1.14	0.34	1.098	1.092	4.428	0.434	1.14	0.34	1.098×10^{-2}	1.092×10^{-2}

Table 2 Parameters of Al₃Ti in JH-2 constitutive equation

ρ	E/GPa	A	B	C	M	N	E_{PSI}	T	H_{EL}	P_{HEL}	B_{ETA}	D_1	D_2	K_1	K_2	K_3	FS
3.38	215	0.85	0.31	0.013	0.21	0.29	1.0	0.0022	0.10	0.03049	1.0	0.020	1.85	2.01	2.6	0.0	1.00

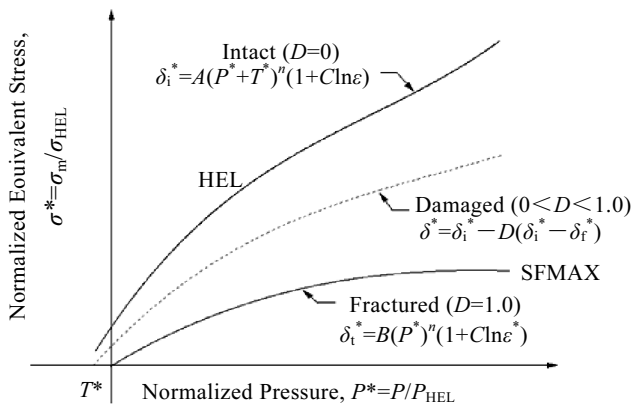


Fig.2 Description of the JH-2 model

The JH-2 constitutive model requires several material constants to completely describe the response of Al₃Ti material. Based on the material deformation, μ (Eq.(9)) and corresponding pressure P (Eqs.(10a) and (10b)) can be calculated.

$$\mu = \rho / \rho_0 - 1 \tag{9}$$

$$P = K_1 \mu + K_2 \mu^2 + K_3 \mu^3 + \Delta P_{n-1} \quad \text{Compression} \tag{10a}$$

$$P = K_1 \mu \quad \text{Tension} \tag{10b}$$

In Eq. (10a), P corresponds to the bulking pressure of the material and is determined by the amount of accumulated damage. Under compressive loading, damage begins to accumulate within the material when the deviator stress exceeds a critical value. This damage accumulation is tracked via a damage parameter (ranging from 0 to 1.0). The pressure is normalized by the equivalent pressure at the HEL. When subjected to tensile pressure, the material responds elastically until brittle failure at a specified effective stress value. This corresponds to complete instantaneous damage.

The numerical method and material properties are validated by the ballistic impact test in Ref.[9]. In order to be consistent with the experiment, the initial velocity of the projectile was set as 900 m/s. The numerically predicted penetration depth is 10.3 mm, which is close to the experiment result of 10.0 mm, thus representing a

reasonable correlation between the experimental and numerical results. A comparison is made between the experimental and simulation results, as shown in Fig. 3. It is clearly seen that the deformation modes, damage range and failure mechanisms of the simulation results are almost consistent with those of the experimental results. This can further guarantee the accuracy of the simulations. All the simulations performed in this work reach a good balance of energy. Thus, the simulation results are reliable.

2 Results and Discussion

2.1 Stress distribution in Ti-Al₃Ti composite

The stress state in Ti-Al₃Ti MIL composite armor during projectile-target interaction process is a very important phenomenon which closely relates to the fracture and penetration resistance of the armor plate. Fig.4 shows the stress distributions at the penetration time of 4.9983 μ s. It is clear that the MIL composite target is mostly under tensile stress state except for the little area in front of the projectile under the compressive stress. The reason is that when the

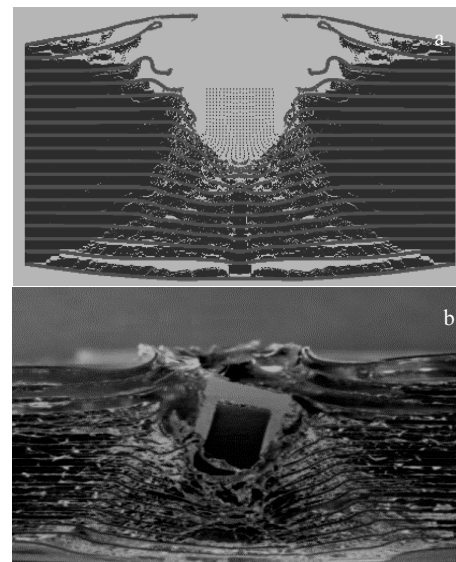


Fig.3 Comparison of the results of Ti/Al₃Ti MIL composites under ballistic impact: (a) numerical simulation and (b) ballistic impact test

projectile penetrates the composite target, the compressive wave will appear and propagate rapidly toward the rear face of the composite target. However, most of the compressive wave will be reflected back as a tensile wave when the compressive wave reaches the interface between the ductile metal Ti and the intermetallic Al_3Ti .

It can also be seen from Fig.4 that the maximum tensile stress in the Ti- Al_3Ti MIL composite target is 27.24 or 33.71 MPa, which is lower than the tensile strength 200 MPa of Ti- Al_3Ti MIL composites. Thus, in the Ti- Al_3Ti MIL composite, there is no micro-crack initiation due to the low tensile stress, and the Al_3Ti layer in front of the projectile are crushed under the compressive stress and show up a high density of micro-cracks. Cao et al.^[12] simulated the shear stress distribution in the composite target when the projectile penetrates the Ti- Al_3Ti MIL composite target, and drew the same conclusion.

2.2 Damage evolution of the composite target

Fig.5 shows the damage evolution of the MIL composite target that is penetrated by a tungsten alloy projectile with an impact velocity of 900 m/s. The tungsten alloy projectile impacts on the MIL composite target, and produces a crater and Al_3Ti fragments. The Ti layer prevents the Al_3Ti fragments ejecting effectively from the crater, and forced the fragments to act with the projectile, which dissipate most of the kinetic energy of projectile and decelerate the projectile.

The simulated image at 10 μs (Fig.5a) obviously shows that a crater is formed on the top surface of the MIL composite target. Moreover, a crack concentration zone exists between the projectile and the composite target, and there is almost no cracking beyond the crack concentration area. When the tungsten alloy projectile penetrates the MIL composite target, the front end of the tungsten alloy projectile is squeezed by the MIL composite target, and the high normal contact stress occurs in the region between the projectile and the composite target. The normal contact stress is higher than the compressive strength of Al_3Ti , which result in the crushing of Al_3Ti phase.

At 15 μs , there are a few vertical cracks originally occurring on the sixth, seventh and eighth layers, as shown in Fig.5b. Such a unique failure feature is observed only in the MIL composite under high velocity impact. Tan^[18] also researched that when the tensile stress, caused by the deflection of the support plate, exceeds the composite target strength, the petal cracks will occur in the bottom surface of support plate. Several studies^[19,20] also demonstrated that in MIL composites the failure always initiated from the Al_3Ti intermetallic compound as transverse brittle cracks appear under quasi-static or fatigue loading.

In the period of 20~50 μs (Fig.5c~5e), with the penetrating of the projectile, transverse, inclined, and vertical cracks are formed in Al_3Ti phase under the combined effect of tensile and compressive stress. The brittle micro-cracks density

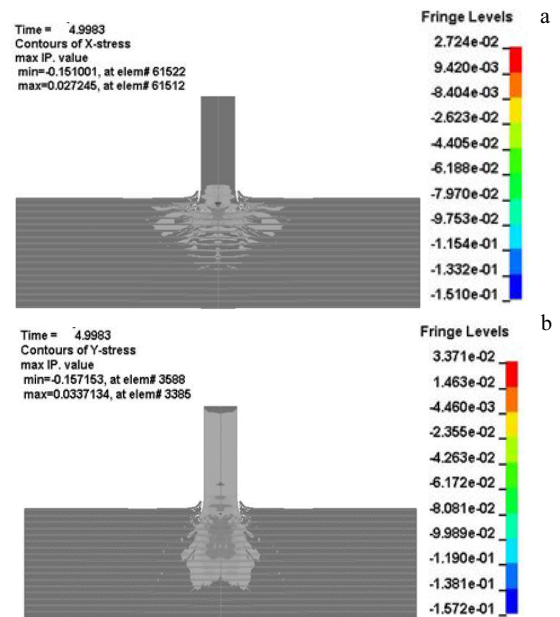


Fig. 4 Stress distribution in the Ti- Al_3Ti composite at 4.9983 μs : (a) x-stress distribution with 900 m/s and (b) y-stress distribution with 900 m/s

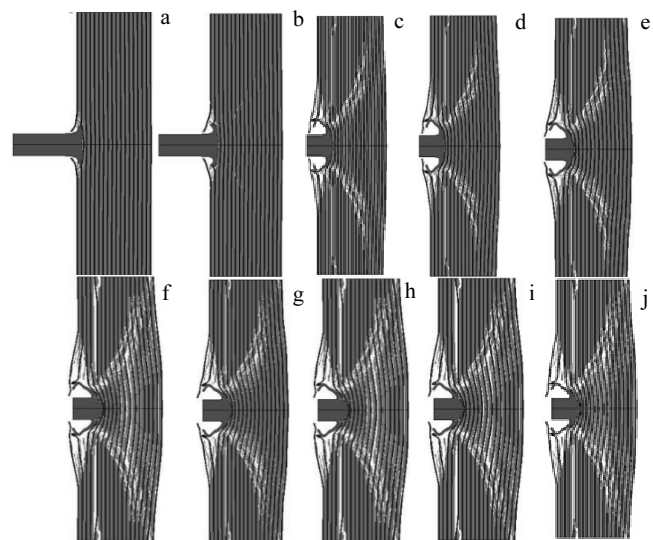


Fig. 5 Damage evolution of target impacted by a tungsten projectile: (a) 10 μs , (b) 15 μs , (c) 30 μs , (d) 45 μs , (e) 50 μs , (f) 60 μs , (g) 65 μs , (h) 70 μs , (i) 75 μs , and (j) 80 μs

increases with time, and these brittle micro-cracks grow into the main crack propagating along an inclined angle direction. In other words, a conoid crater occurs in the target. The angle of conoid is about 60 degree, which agrees with the results in Refs.[19,20].

During the final penetration time of 60~80 μs (Fig. 5f~5j), the delamination cracks occur continuously between the main

cracks under the reflected tensile stress wave. The depth and diameter of the ceramic cone is becoming smaller and smaller until the penetration process is over. The projectile penetrates into the ceramic conoid, which also results in producing new small ceramic conoid, which is also mentioned in Ref.[20]. Such penetration will repeat until the diameter of the new small ceramic conoid is close to the diameter of projectile. Then, the new small ceramic conoid is compressed by the projectile and separated from the surrounding ceramic fragments. Cheng et al.^[21] also found that the final penetration zone is dominated by the delamination cracks.

2.3 Residual speed and kinetic energy of the projectile

Fig. 6 shows the residual speed and kinetic energy of the tungsten alloy projectile as functions of time when the tungsten alloy projectile penetrates into the monolithic intermetallic Al_3Ti and $\text{Ti-Al}_3\text{Ti}$ composites. It is noted that in the early ballistic impact period (0~15 μs), the residual speed and kinetic energy of the tungsten alloy projectile penetrating into the two targets have similar variation tendency. At the second stage (15~50 μs), the residual speed and kinetic energy of the tungsten alloy a projectile in the $\text{Ti-Al}_3\text{Ti}$ decrease faster than that in the Al_3Ti target. During the final penetration period (after ~50 μs), the residual speed of the tungsten alloy projectile penetrating the monolithic intermetallic Al_3Ti and $\text{Ti-Al}_3\text{Ti}$ are 280 and 0 m/s, respectively. The kinetic energy of the tungsten alloy projectile penetrating the monolithic intermetallic Al_3Ti and $\text{Ti-Al}_3\text{Ti}$ are 460 and 0 J, respectively. The residual speed and

kinetic energy of the tungsten alloy projectile keep steady. The comparison clearly shows that MIL composites possess superior penetration resistance over the intermetallic Al_3Ti . The results indicate that there is a significant increase in energy absorption by adding layers of Ti in Al_3Ti ^[22].

3 Conclusions

1) The stress distribution, penetration process, and failure mechanism of $\text{Ti-Al}_3\text{Ti}$ in the penetration process impacted by the tungsten projectile is studied. When it is impacted by a tungsten projectile at 900 m/s, the metal-intermetallic laminate composite target mainly suffers from tensile stress, since the compressive wave is reflected back as a tensile wave when the compressive wave reaches the interface between the ductile metal Ti and the intermetallic Al_3Ti . In the penetration period of 20~50 μs , the transverse, inclined, and vertical cracks are formed in Al_3Ti phase under the combined effect of tensile and compressive stress, and these cracks dramatically absorb the kinetic energy of the projectile.

2) The penetration resistance of $\text{Ti-Al}_3\text{Ti}$ is higher than that of the Al_3Ti target, which indicates that there is a significant increase in energy absorption by adding layers of Ti in Al_3Ti .

References

- 1 Harach D J, Vecchio K S. *Metall MaterTrans A*[J], 2001, 32: 1493
- 2 Han Y, Lin C, Han X et al. *Materials Science and Engineering A*[J], 2017, 688: 338
- 3 Cao Y, Guo C H, Zhu S F et al. *Material Science and Engineering A*[J], 2015, 637: 235
- 4 Zelepugin S A, Shpakov S S. *Journal of Composite Mechanics and Design*[J], 2009, 15: 369
- 5 Zhou P J, Guo C H, Wang E H et al. *Material Science and Engineering A*[J], 2016, 665: 66
- 6 Jiang F, Kulin R M, Vecchio K S. *Journal of the Minerals Metals and Materials Society*[J], 2010, 62: 35
- 7 Rohatgi A, Harach D J, Vecchio K S et al. *Acta Materialia*[J], 2003, 51: 2933
- 8 Guo Y, Shi Z, Xu Y et al. *Rare Metal Materials and Engineering* [J], 2014, 43: 813
- 9 Harach D J. *Thesis for Doctorate*[D]. Los Angeles: University of California, 2000
- 10 Randow C, Gazonas G. *7th World Congress on Computational Mechanics*[C]. Los Angeles: CCM, 2006
- 11 Zelepugin S, Mali V, Zelepugin A et al. *American Physical Society*[J], 2012, 1426: 1119
- 12 Cao Y, Zhu S F, Guo C H et al. *Applied Composite Materials*[J], 2015, 22: 437
- 13 Leseur D R. *Experimental Investigations of Material Models for Ti-6Al-4V Titanium and 2024-T3 Aluminum*. DOT/FAA/AR-00/25[R], US: Department of Transportation, Federal

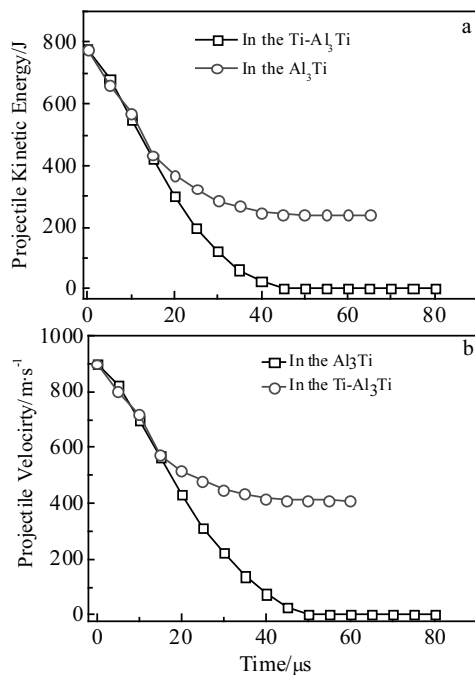


Fig. 6 Variations of projectile kinetic energy (a) and projectile velocity (b)

- Aviation Administration, 2000
- 14 Fan X L, Suo T, Wang T J. *Acta Mechanica Solida Sinica*[J], 2013, 26: 111
- 15 Cronin D S, Bui K, Kaufmann C et al. *4th European LS-Dyna Users Conference*[C]. Ulm, Germany: ELSDU, 2003: 47
- 16 Li T, Grignon F, Benson D et al. *Material Science and Engineering A*[J], 2004, 374: 10
- 17 Holmquist T J, Johnson G R. *International Journal of Impact Engineering*[J], 2005, 31: 113
- 18 Tan Z H, Han X, Zhang W et al. *International Journal of Impact Engineering*[J], 2010, 37: 1162
- 19 Sherman D, Ben-Shushan T. *International Journal of Impact Engineering*[J], 1998, 21: 245
- 20 Fellows N A, Barton P C. *International Journal of Impact Engineering*[J], 1999, 22: 793
- 21 Cheng W L, Langlie S, Itoh S. *International Journal of Impact Engineering*[J], 2003, 29: 167
- 22 Yahaya R, Sapuan S M, Jawaid M et al. *Measurement*[J], 2016, 77: 335

强冲击载荷下 Ti-Al₃Ti 金属间化合物复合材料失效机理研究

范学领¹, 原梅妮², 秦强³

(1. 西安交通大学 机械结构强度与振动国家重点实验室, 陕西 西安 710049)

(2. 中北大学, 山西 太原 030051)

(3. 中航工业飞机强度研究所, 陕西 西安 710065)

摘要: 以数值研究了破片冲击载荷作用下 Ti-Al₃Ti 金属间化合物复合材料的动力学行为及其失效机理。系统考察了强冲击载荷下, Ti-Al₃Ti 金属间化合物复合材料的冲击性能、应力分布、失效行为及能量吸收机制。结果表明: 在冲击载荷作用下, 压缩波在复合材料间由于界面反射转变为拉伸波, 导致 Ti-Al₃Ti 金属间化合物复合材料主要处于拉应力状态。在破片贯穿金属间化合物复合材料的中间阶段, 在 Al₃Ti 内形成横向裂纹、倾斜裂纹和垂直裂纹, 这些破坏模式可有效地吸收冲击动能。因而, Ti-Al₃Ti 金属间化合物复合材料具有优异的动力学吸能特性。

关键词: 金属间化合物复合材料; 有限元; 高速冲击; 失效

作者简介: 范学领, 男, 1978 年生, 博士, 教授/博导, 西安交通大学航天航空学院机械结构强度与振动国家重点实验室, 陕西 西安 710049, 电话: 029-82667864, E-mail: fanxueling@mail.xjtu.edu.cn